



# Exploration of Nonlinear Optical Properties of Triphenylamine-Dicyanovinylene Coexisting Donor- $\pi$ -Acceptor Architecture by the Modification of $\pi$ -Conjugated Linker

## OPEN ACCESS

### Edited by:

Ashok Kumar,  
National Physical Laboratory (CSIR),  
India

### Reviewed by:

Mohammad Chahkandi,  
Hakim Sabzevari University, Iran  
Hossein Asghar Rahnamaye Aliabad,  
Hakim Sabzevari University, Iran

### \*Correspondence:

Muhammad Khalid  
muhammad.khalid@kfueit.edu.pk  
Khalid@iq.usp.br  
Yang Jiang  
yangjiang1st@yeah.net  
Changrui Lu  
crlu@dhu.edu.cn

### Specialty section:

This article was submitted to  
Quantum Materials,  
a section of the journal  
Frontiers in Materials

Received: 03 June 2021

Accepted: 08 July 2021

Published: 12 August 2021

### Citation:

Khan MU, Khalid M, Asim S, Momina, Hussain R, Mahmood K, Iqbal J, Akhtar MN, Hussain A, Imran M, Irfan A, Ali A, Rehman MFur, Jiang Y and Lu C (2021) Exploration of Nonlinear Optical Properties of Triphenylamine-Dicyanovinylene Coexisting Donor- $\pi$ -Acceptor Architecture by the Modification of  $\pi$ -Conjugated Linker. *Front. Mater.* 8:719971. doi: 10.3389/fmats.2021.719971

Muhammad Usman Khan<sup>1</sup>, Muhammad Khalid<sup>2\*</sup>, Sumreen Asim<sup>2</sup>, Momina<sup>2</sup>, Riaz Hussain<sup>1</sup>, Khalid Mahmood<sup>3</sup>, Javed Iqbal<sup>4</sup>, Muhammad Nadeem Akhtar<sup>5</sup>, Amjad Hussain<sup>1</sup>, Muhammad Imran<sup>6</sup>, Ahmad Irfan<sup>6</sup>, Akbar Ali<sup>7</sup>, Muhammad Fayyaz ur Rehman<sup>7</sup>, Yang Jiang<sup>8\*</sup> and Changrui Lu<sup>9\*</sup>

<sup>1</sup>Department of Chemistry, University of Okara, Okara, Pakistan, <sup>2</sup>Department of Chemistry, Khwaja Fareed University of Engineering and Information Technology, Rahim Yar Khan, Pakistan, <sup>3</sup>Institute of Chemical Sciences, Bahauddin Zakariya University, Multan, Pakistan, <sup>4</sup>Department of Chemistry, University of Agriculture, Faisalabad, Pakistan, <sup>5</sup>Division of Inorganic Chemistry, Institute of Chemistry, Baghdad-ul-Jadeed Campus, The Islamia University of Bahawalpur, Bahawalpur, Pakistan, <sup>6</sup>Department of Chemistry, Faculty of Science, King Khalid University, Abha, Saudi Arabia, <sup>7</sup>Department of Chemistry, University of Sargodha, Sargodha, Pakistan, <sup>8</sup>Department of Urology, Jiading Branch of Shanghai General Hospital, Shanghai Jiao Tong University School of Medicine, Shanghai, China, <sup>9</sup>Department of Chemistry, Chemical Engineering and Biotechnology, Donghua University, Shanghai, China

High-tech electronic, optics, and storage devices require organic compounds with nonlinear optical (NLO) properties. This study designed D- $\pi$ -A based dyes with donor triphenylamine (TPA) and acceptor dicyanovinylene (DCV) species by structurally modifying  $\pi$ -conjugated linkers. Our density functional theory (DFT) computations analyzed the impact of structural variations on the nonlinear optical (NLO) response of newly designed dyes. The B3LYP/6-31G(d,p) level determined the quantum chemical insights: frontier molecular orbital (FMOs), natural bond orbitals (NBOs), and nonlinear optical (NLO) properties of the designed dyes (DPTM-1 to DPTM-12). UV-Vis analysis based on the TD-DFT/CAM-B3LYP/6-311+G(d,p) level explored the optoelectronic properties. **DPTM-1** and **DPTM-5** showed the highest red-shifted absorption band at 519 and 506 nm. NBO analysis shows that DPTM-1 to DPTM-12 dyes have positive values for all donors (D) and  $\pi$ -spacers but negative values for acceptors (A). The  $\pi$ -spacers act as a conveyor between donor and acceptor moieties; thus, electrons were transferred smoothly from D to A units, which resulted in a charge separation state. Our calculations show the extent of NLO response in terms of electronic transitions, polarizability  $\langle\alpha\rangle$ , and first hyperpolarizability ( $\beta$ ) values. The highest value of  $\beta_{total}$  was 110,509.23 a.u. manifested in **DPTM-6** due to 2,5-dimethyloxazole as a second  $\pi$ -linker, twice that of **R** (66,275.95 a.u.). Also, **DPTM-6** and **DPTM-8** exhibit the lowest energy band gap of 2.06 and 2.04 eV, respectively. In short, all DPTM-1 to DPTM-12 dyes manifested maximum absorption, lowest energy band gap, greater charge transfer from donor to the acceptor, and better first hyperpolarizability

values as compared to the R and showed good NLO response. The present work represents new compounds with remarkable NLO properties and their applications in modern high-tech devices.

**Keywords:** nonlinear optical properties,  $\pi$ -conjugated linkers, density functional theory, metal-free organic dyes, triphenylamine-dicyanovinylene

## INTRODUCTION

With the rapid rise of high-tech electronic, optics, and storage devices, organic compounds with NLO properties gained unparalleled popularity and dominance in various disciplines, such as medicine, material science, atomic, molecular, and solid-state physics, surface interface sciences, and chemical dynamics (Eaton, 1991; Peng and Yu, 1994; Tsutsumi et al., 1998; Breitung et al., 2000; Christodoulides et al., 2010). Organic NLO materials, especially with larger  $\pi$ -extended frames, are significantly interesting as dynamic intermolecular charge transfer (ICT) materials with excellent NLO response, facile synthesis, optical switching, frequency shifting, and better signal reception. The presence of delocalized electrons in the organic compounds leads to further enhancement in the NLO response (Anthony et al., 2008; Yamashita, 2011; Ivanov et al., 2013; Khoo, 2014). A significant amount of NLO responses has been observed in organic compounds due to  $\pi$ -electrons with strong electric polarization, low dielectric coefficient, quick response, and high laser damage threshold and  $\pi$ -bond system involves charge distribution from donor to acceptor (Sung and Hsu, 1998; Hochberg et al., 2006). Intermolecular charge transfer occurs from electron-donating to the electron-withdrawing units by the  $\pi$ -conjugated linkers directly linked with the first hyperpolarizability ( $\beta$ ) (Zyss, 1987; Prasad and Williams, 1991; Drozd and Marchewka, 2005; Janjua, 2017).

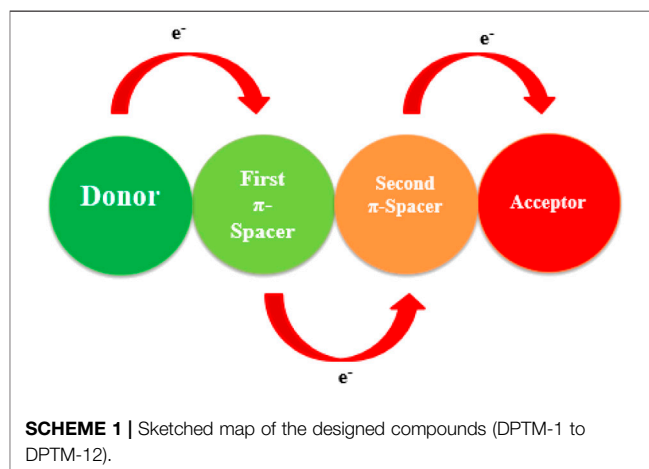
HOMO and LUMO allow charge transfer, but the  $\pi$ -conjugated system leads to charge transfer in an electric field where the  $\pi$ -spacer is a basic molecule (Datta and Pal, 2005; Siddiqui et al., 2012; Garza et al., 2014). By changing the conjugation system the properties of dyes can vary and the NLO response can improve by choosing the finest length of conjugation. Appropriate arrangement of donor, acceptors, and  $\pi$ -bridge plays a crucial role in designing a competent organic compound (Dalton, 2001; Dalton, 2002). This appropriate arrangement enhances the electronic distribution, induces charge separation, increases absorption range towards longer wavelength, reduces charge recombination, and decreases the HOMO-LUMO energy gap, resulting in an improved NLO response. There are large dipole moments between the ground and excited state of the compounds because of ICT, including electron density transfer from D to A units through  $\pi$ -bridge (Haid et al., 2012; Srinivasan et al., 2017). Literature has shown that NLO response can be improved when ICT is enhanced by ring twisting and optimizing the D-A pair (Dulcic et al., 1981; Berkovic et al., 1987). The organic dyes with  $\pi$ -bond system involved delocalization of charge. The major effect of  $\pi$ -bridge on NLO activity is also important in the prediction of optimized NLO properties. Although D units have a major impact on NLO

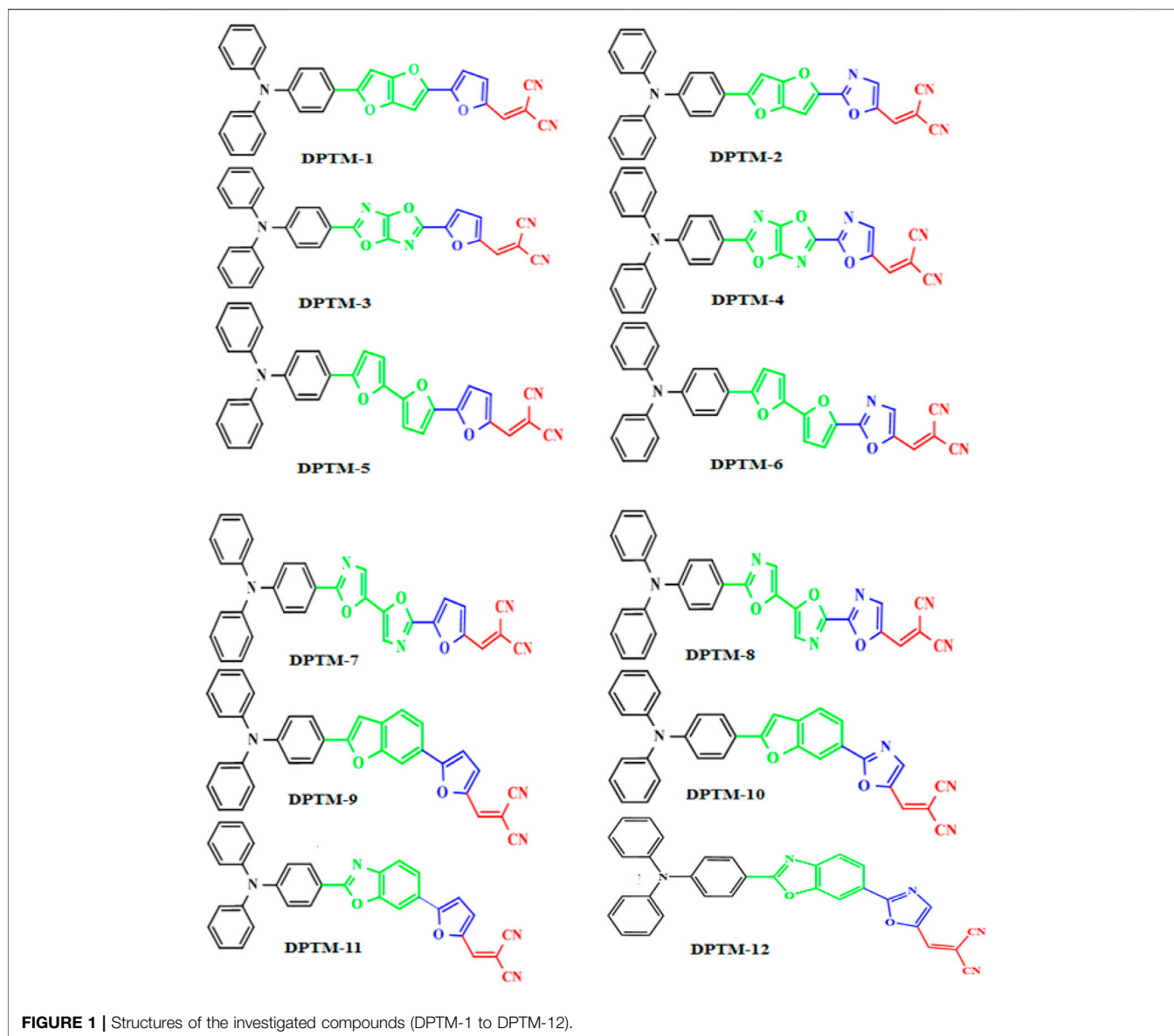
properties, one cannot ignore the role of the acceptor unit. Different types of  $\pi$ -spacers are helpful in a good connection between HOMO and LUMO units to have a good NLO response (Khan et al., 2018a).

Literature is overflowing with various designs comprising A- $\pi$ -D- $\pi$ -A, D-A, D- $\pi$ -A, D- $\pi$ -A- $\pi$ -D, D-A- $\pi$ -A, D- $\pi$ - $\pi$ -A, and D-D- $\pi$ -A (Khalid et al., 2020). It has been determined by both experimental and theoretical inspection that D- $\pi$ -A types of designed dyes show excellent NLO responses (Khan et al., 2018b). Furthermore, the optimal length of  $\pi$ -conjugation, composited in between donor and acceptor, also contributes to an increased NLO response (Saead et al., 2020). That is why, in this study, we have tailored the  $\pi$ -conjugated system and designed the D- $\pi$ -A type of compounds (DPTM-1 to DPTM-12). To the best of our knowledge, these compounds have never been designed before for the efficient theoretical study for NLO properties.

## COMPUTATIONAL PROCEDURE

In the present study, NBO analysis, electronic structures, absorption spectra, and NLO properties of D- $\pi$ -A dyes were calculated by performing density functional theory and time-dependent density functional theory. All computational calculations were performed using Gaussian 09 package program (Olson and Boldyrev, 2012). Ground state geometry optimization of the dyes is determined in the gas phase to confirm that no imaginary frequencies are involved in dyes through the B3LYP (Civalleri et al., 2008) level of theory combined with a 6-31G(d,p) (Afzal et al., 2020; Bilal Ahmed Siddique et al., 2020; Hussain et al., 2020; Mehboob et al., 2020) basis set. The HOMO-





LUMO energies and their differences were calculated using the same function. FMO investigation proved highly beneficial in understanding electronic transitions from donor to the acceptor orbital. The charge transfer interactions in the entitled compounds were observed in the NBO analysis. TD-DFT calculations with the CAM-B3LYP/6-311+G(d,p) level were used to comprehend the UV-Visible absorption spectra of the entitled molecules (Yanai et al., 2004). All input files were made by Gauss View 5.0 (Vural et al., 2017), whereas output effects were construed and visualized using Gauss View, Avogadro (Hanwell et al., 2012), and Chemcraft (Dena et al., 2019) programs. The Gaussian output presented six linear polarizability tensors ( $\alpha_{xx}$   $\alpha_{yy}$   $\alpha_{zz}$   $\alpha_{xy}$   $\alpha_{xz}$   $\alpha_{yz}$ ) and ten first hyperpolarizability tensors ( $\beta_{xxx}$   $\beta_{xyy}$   $\beta_{xzz}$   $\beta_{yyy}$   $\beta_{xyx}$   $\beta_{yzz}$   $\beta_{zzz}$   $\beta_{xxz}$   $\beta_{yyz}$   $\beta_{xyz}$ ) along the  $x$ ,  $y$ , and  $z$  directions, respectively. Polarizabilities and first hyperpolarizability values of the design

compounds (DPTM-1 to DPTM-12) have been calculated at the same level of theory. **Equations 1** and **2** can be utilized for calculating the polarizability  $\langle\alpha\rangle$  and first hyperpolarizability ( $\beta_{total}$ ) of the entitled compounds (Karakas et al., 2007).

$$\langle\alpha\rangle = -\frac{1}{3}(\alpha_{xx} + \alpha_{yy} + \alpha_{zz}) \quad (1)$$

$$\beta_{total} = \left[ (\beta_{xxx} + \beta_{yyy} + \beta_{zzz})^2 + (\beta_{yyy} + \beta_{yzz} + \beta_{yxz})^2 + (\beta_{zzz} + \beta_{zxx} + \beta_{zyz})^2 \right]^{1/2} \quad (2)$$

## RESULTS AND DISCUSSION

Khan *et al.* modified a D- $\pi$ -A-based 2-((5-(2-(4-(diphenylamino)phenyl)benzo[d]thiazol-5-yl)thiophen-2-yl)methylene)malononitrile dye (**R**) by changing  $\pi$ -conjugated linkers between the fixed donor

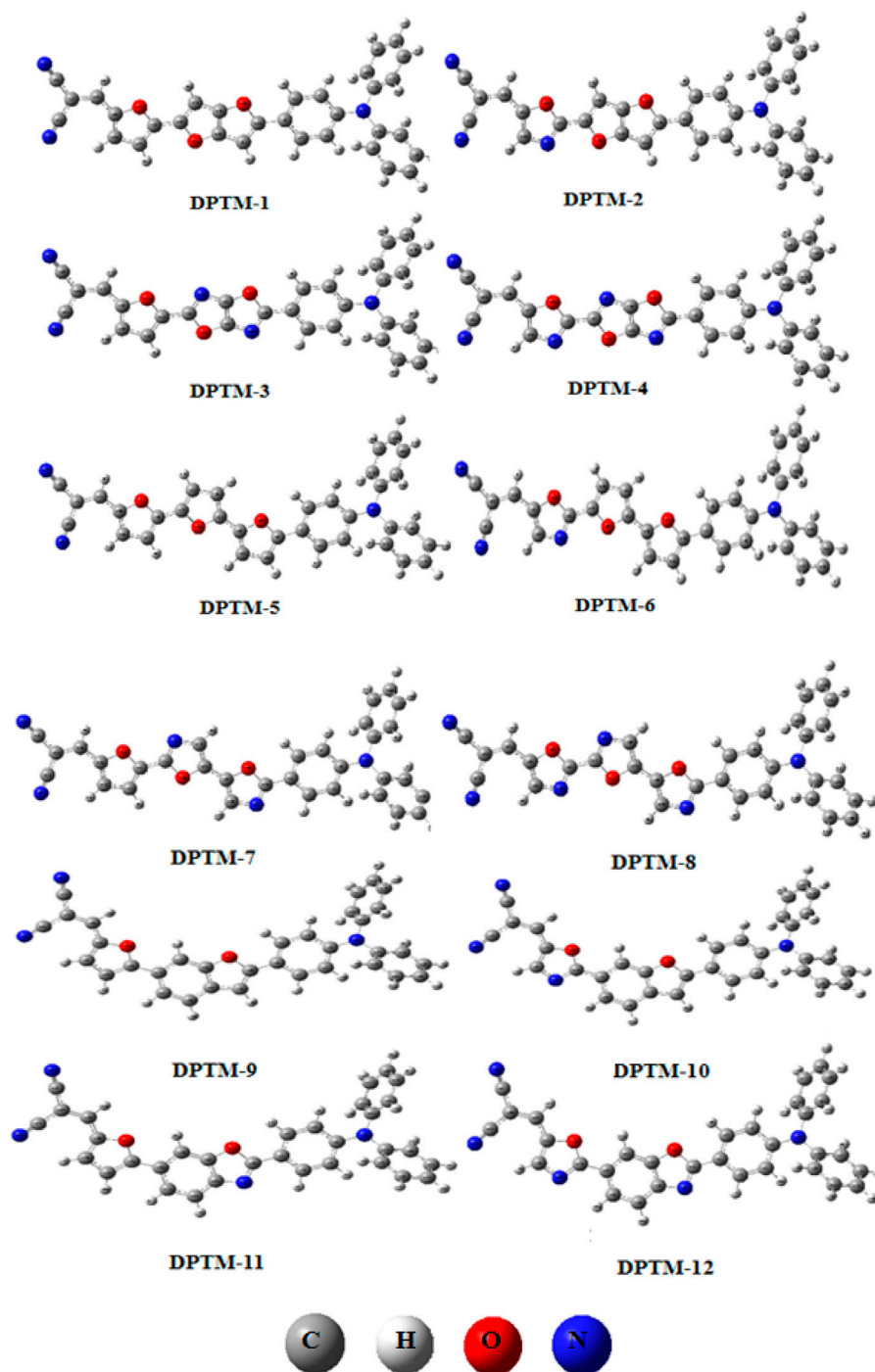


**FIGURE 2** | Optimized structures of the investigated compounds (DPTM-1 to DPTM-12).

(triphenylamine) and acceptor (dicyanovinylene) species to enhance its NLO properties (Khan et al., 2018a). In this present work, eight  $\pi$ -linkers that were not previously reported are used to design organic dye with potential NLO responses. The molecular and optimized structures of the entitled dyes, as shown in **Figures 1, 2**, have three fragments, D,  $\pi$ -spacer, and A. In the designed

compounds (DPTM-1 to DPTM-12), triphenylamine (TPA) acts as a donor and dicyanovinylene (DCV) as an acceptor unit with various  $\pi$ -conjugated linkers. Various combinations were made to design twelve new TPA-DCV based D- $\pi$ -A compounds involving six  $\pi$ -spacers used as first  $\pi$ -linkers and two  $\pi$ -spacers as second  $\pi$ -linkers. To judge the impact of structural changes on NLO

**TABLE 1** | The  $E_{HOMO}$ ,  $E_{LUMO}$ , and energy gap ( $E_{LUMO}-E_{HOMO}$ ) of investigated compounds (DPTM-1 to DPTM-12).

Compounds	$E_{HOMO}$	$E_{LUMO}$	$\Delta E$
DPTM-1	-5.405	-3.170	2.24
DPTM-2	-5.521	-3.324	2.19
DPTM-3	-5.663	-3.427	2.24
DPTM-4	-5.775	-3.574	2.20
DPTM-5	-5.342	-3.174	2.17
DPTM-6	-5.405	-3.341	2.06
DPTM-7	-5.604	-3.438	2.17
DPTM-8	-5.645	-3.608	2.04
DPTM-9	-5.496	-3.112	2.38
DPTM-10	-5.572	-3.292	2.28
DPTM-11	-5.675	-3.185	2.49
DPTM-12	-5.743	-3.366	2.38

Units in eV.

properties, density functional theory (DFT) and time-dependent density functional theory (TD-DFT) calculations were performed.

## ELECTRONIC STRUCTURE

The FMO analysis is considered a standard approach to predict the chemical stability in molecules (Gunasekaran et al., 2008). The frontier molecular orbitals, *i.e.*, HOMO (highest occupied molecular orbital) and LUMO (lowest unoccupied molecular orbital), play an exceptional role in the absorption spectra and mechanical illustration of the compounds. Usually, HOMO is referred to as an electron donator, while LUMO is usually regarded as an acceptor (Amiri et al., 2016). Band gap ( $E_{LUMO}-E_{HOMO}$ ) is considered an exceptional factor in predicting hardness, strength, softness, dynamic stability, and chemical reactivity of the deliberated dyes (Khalid et al., 2017), where a sizeable band gap shows minimum reactivity and maximum stability and hardness of a molecule. In contrast, highly reactive and soft molecules, predicted with a small  $E_{LUMO}-E_{HOMO}$  band gap, are far more polarized and serve as a finer competitor in offering the best NLO response (Parr et al., 1999; Lesar and Milošev, 2009; Chattaraj et al., 2011).  $E_{HOMO}$ ,  $E_{LUMO}$ , and bandgap ( $E_{LUMO}-E_{HOMO}$ ) for DPTM-1 to DPTM-12 have been determined by the DFT computational analysis. The calculated values are given in **Table 1**.

It is observed that all the designed dyes tend to show relatively low band gaps than the reference (**R**), *i.e.*, 2.4 eV (Khan et al., 2018a), which manifests a remarkable outcome of the used  $\pi$ -conjugates in HOMO-LUMO transition states. The increasing energy gap order of **R** and DPTM-1 to DPTM-12 is observed as **DPTM-8**<**DPTM-6**<**DPTM-7**<**DPTM-5**<**DPTM-2**<**DPTM-4**<**DPTM-1**<**DPTM-3**<**DPTM-10**<**DPTM-12**<**DPTM-9**<**R**<**DPTM-11** (**Table 1**).

The HOMO-LUMO band gap in **DPTM-8** is the least among all dyes, *i.e.*, 2.04 eV due to first  $\pi$ -linker 2,2'-dimethyl-5,5'-bioxazole and second  $\pi$ -linker 2,5-dimethyloxazole. These two  $\pi$ -conjugated linkers have provided a better bridge for transferring electrons from the TPA to DCV.  $\Delta E$  of **DPTM-11** was found greater than 2.49 eV. The first and second  $\pi$ -linkers

2,5-dimethylbenzo[d]oxazole and 2,5-dimethylfuran, used in **DPTM-11**, have interrupted the transfer of electrons from the TPA to DCV (**Figures 1, 2**). That is why **DPTM-11** has shown the highest band gap among all the designed dyes. These smaller band gaps have shown favorable NLO properties. The HOMO-LUMO (+1, -1, +2, -2) value and band gaps are mentioned in the supplementary information (**Supplementary Table 13** and **Supplementary Figure 1**). The structural display of HOMO-LUMO orbitals with electron density distribution pattern is shown in **Figure 3**. In HOMO, the orbital electron density is mainly exhibited on the donor TPA and partially present along with first  $\pi$ -linkers. In the case of LUMO, the electron density predominantly occurred on the acceptor side DCV and is slightly present along with second  $\pi$ -linkers. This revealed the charge transfer from donor to acceptor moieties and illustrated the enhanced properties of NLO materials. Structural modifications by changing the  $\pi$ -conjugated linkers exhibited remarkable results for NLO resources.

## GLOBAL REACTIVITY PARAMETERS

The bandgap ( $E_{LUMO}-E_{HOMO}$ ) is crucial in describing the global reactivity parameters such as global hardness ( $\eta$ ), global softness ( $\sigma$ ), global electrophilicity index ( $\omega$ ), electron affinity ( $EA$ ), ionization potential ( $IP$ ) (Fukui, 1982), electronegativity ( $X$ ), and the chemical potential ( $\mu$ ) (Parr et al., 1978) and calculated by utilizing Koopmans's theorem (Koopmans, 1934) equations.

$$IP = -E_{HOMO} \quad (3)$$

$$EA = -E_{LUMO} \quad (4)$$

$$X = \frac{[IP + EA]}{2} = \frac{[E_{LUMO} + E_{HOMO}]}{2} \quad (5)$$

$$\eta = \frac{[IP - EA]}{2} = \frac{[E_{LUMO} - E_{HOMO}]}{2} \quad (6)$$

$$\mu = \frac{E_{HOMO} + E_{LUMO}}{2} \quad (7)$$

$$\sigma = \frac{1}{2\eta} \quad (8)$$

$$\omega = \frac{\mu^2}{2\eta} \quad (9)$$

The outcomes from the equations are represented in **Table 2**.

The electron affinity represents electron-withdrawing ability, while electron-donating tendency can be determined by the ionization potential. Among all the entitled dyes, maximum electron affinity is observed in **DPTM-8**, *i.e.*, 3.61 a.u. while the maximum ionization potential, *i.e.*, 5.775 a.u., is shown by **DPTM-4** (**Table 2**). Electronegativity is a tendency to attract the electron towards itself, while chemical potential ( $\mu$ ) value describes the stability of molecules. A more negative value of chemical potential represents the stability of the molecules. The highest negative value of chemical potential is determined in **DPTM-4** as -4.675. The bandgap and hardness of the molecules have a direct relation. A sizeable bandgap describes a less reactive molecule with greater hardness and high kinetic stability.

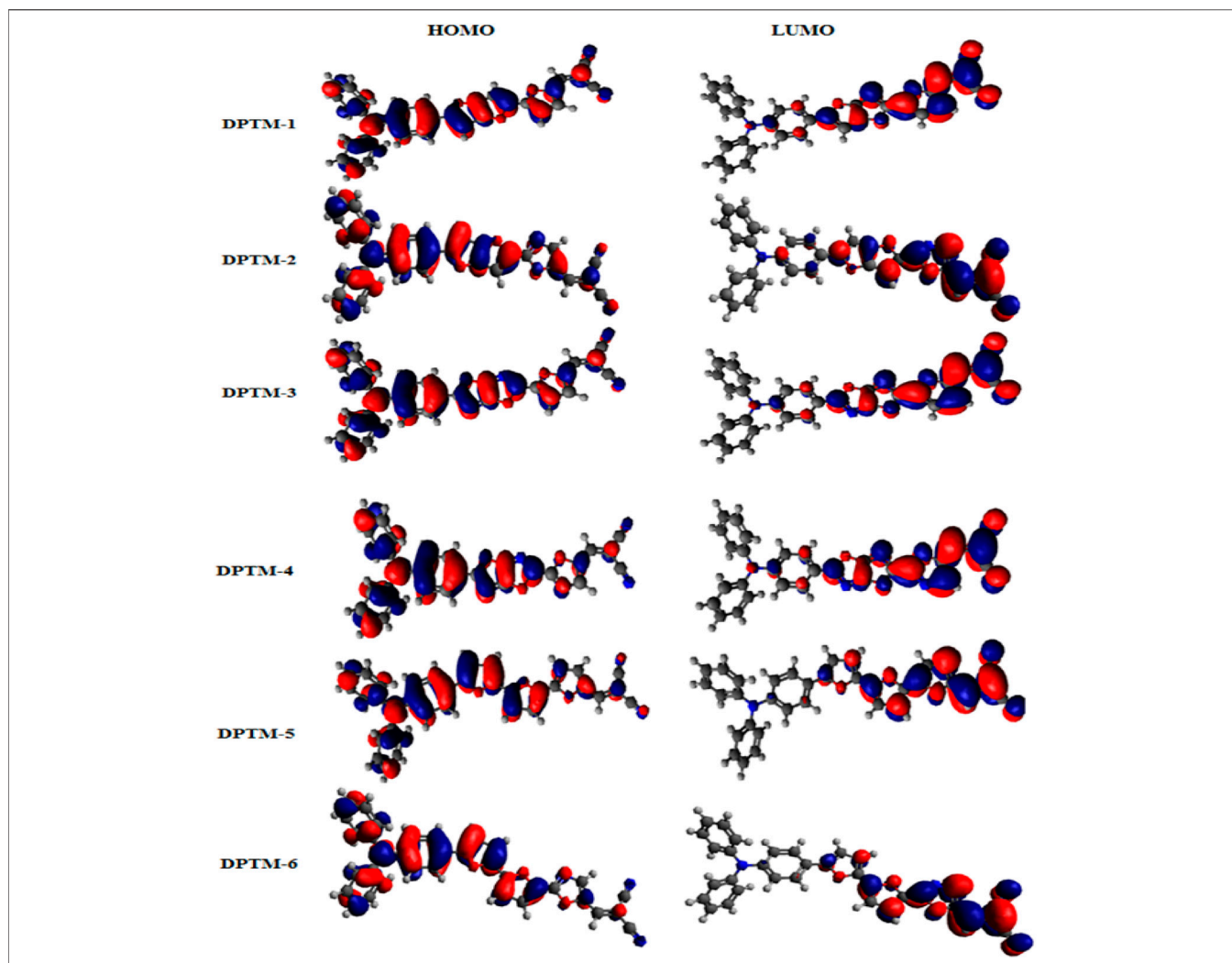


**FIGURE 3** | HOMOs and LUMOs of the studied dyes (DPTM-1 to DPTM-12).

Furthermore, if a molecule has less energy bandgap, it describes the more reactive molecule, with lesser hardness and lower kinetic strength.

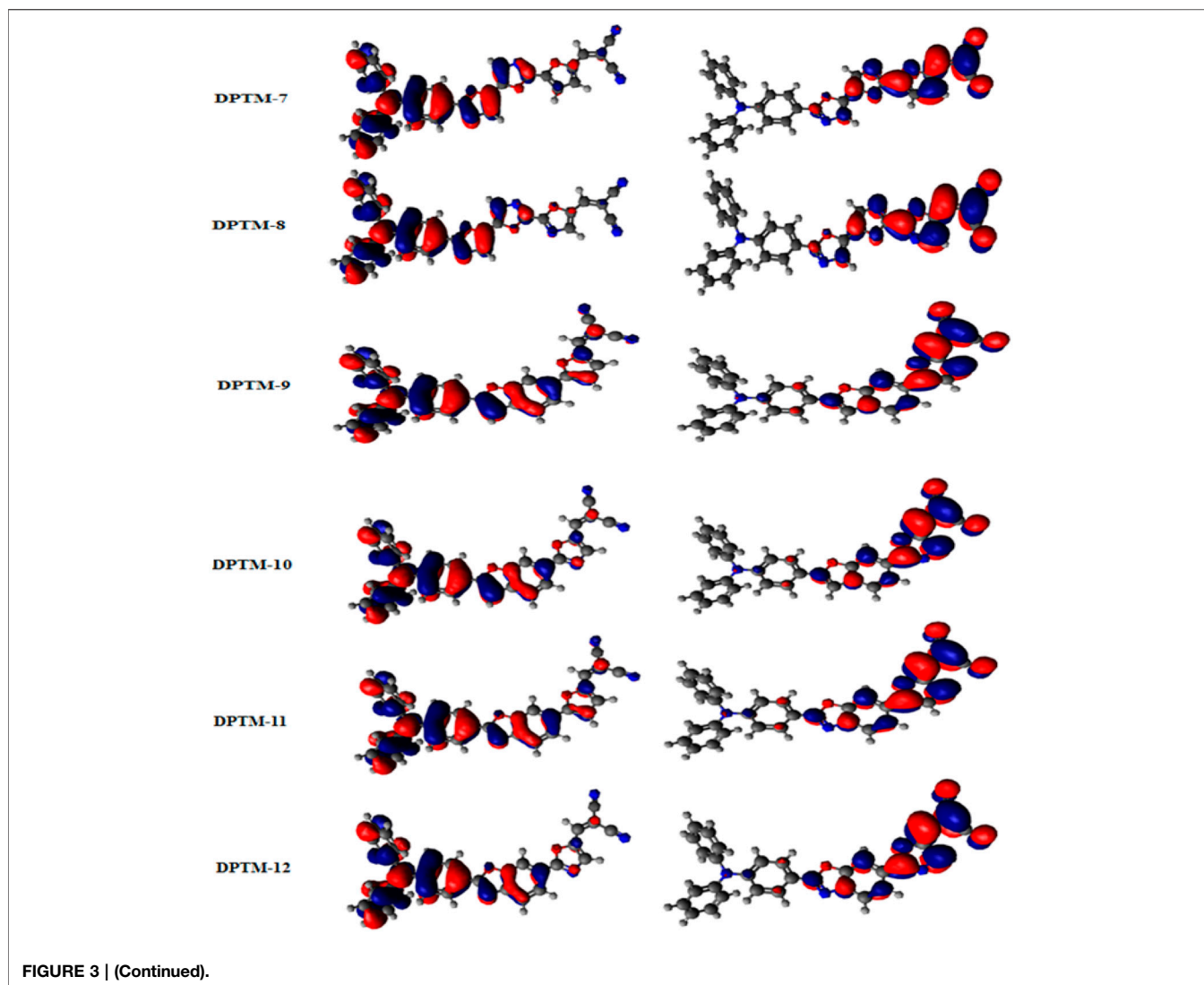
Among all the designed compounds, the lowest hardness value is calculated in **DPTM-6**, *i.e.*, 1.032 *a.u.* In **DPTM-7**, first and second  $\pi$ -conjugated linkers such as 5,5'-dimethyl-2,2'-bifuran and 2,5-dimethyloxazole provided a better path for transfer of electrons from HOMO-LUMO orbital in a minimum amount of energy. The least chemical stability and the maximum hardness are observed in **DPTM-11** as 1.245 *a.u.* The decreasing order of hardness of the investigated molecules is **DPTM-11**>**DPTM-9**>**DPTM-12**>**DPTM-10**>**DPTM-3**>**DPTM-1**>**DPTM-4**>**DPTM-2**>**DPTM-5**>**DPTM-7**>**DPTM-6**> **DPTM-8**.

Softness is another factor that reveals molecule's reactivity as it is directly related to chemical reactivity. In the designed moieties, **DPTM-8** has higher value of softness, 0.49092 *a.u.* The **DPTM-8** has first  $\pi$ -conjugated linkers 2,2'-dimethyl-5,5'-bioxazole and second  $\pi$ -linker 2,5-dimethyloxazole that play a crucial role in

transfer of the electron density from D to A moieties without any barrier. The decreasing order of softness of investigated molecules is **DPTM-8**>**DPTM-6**>**DPTM-7**>**DPTM-5**>**DPTM-2**>**DPTM-4**>**DPTM-1**>**DPTM-3**>**DPTM-10**>**DPTM-12**>**DPTM-9**>**DPTM-11**. Therefore, **DPTM-8** has shown the lowest band gap among all the dyes, showing maximum softness and significant NLO properties.

## NATURAL BOND ORBITAL (NBO) ANALYSIS

NBO is a technique that thoroughly explains the charge transfer and conjugative interactions between the donor and acceptor moieties (James et al., 2006; Szafran et al., 2007). It also provides a steady explanation of intermolecular interactions between two or more counterparts. It is based on the lone pair and bond pair interactions. It is a beneficial technique to study the transmission



of electrons from the D orbital to the A orbital in the D- $\pi$ -A system. The charge transfer of studied compounds findings is expressed in **Table 3**.

It has been observed from **Table 3** that donor units contain a positive charge, due to which it has excellent electron-donating power. However, acceptor moiety holds a negative charge describing that acceptors will accept electrons effectively. The  $\pi$ -spacers have positive charges, demonstrating that they will not stop the electrons transfer and act as a bridge to smoothly transfer charge densities from donor to acceptor units. Transfer of charge from D (filled) orbital to A (vacant) orbital is because of the hyperconjugative and intra- and intermolecular interactions. It has been observed that the highest NBO charge values were observed for **DPTM-1** and the least NBO charge values were observed for **R**. The most suitable push-pull architecture is seen in **DPTM-1**, which is conveying the charge towards  $\pi$ -bridge to act as a conveyor and allowed to pass the charge towards the acceptor unit. The electronic transition types of NBO (DPTM-1 to DPTM-12) are demonstrated in the supplementary information

(**Supplementary Tables 14–25**). Thus, the results prove the successful transfer of charges from filled to vacant orbital through  $\pi$ -spacer. The NBO charge values of other dyes also showed a close relation to each other.

## NONLINEAR OPTICAL (NLO) PROPERTIES

NLO dyes and materials are widely used in communication technology, signal processing optical switches, and memory devices. A thorough understanding of NLO properties is required for the design of these materials. Electronic properties are measured to be accountable for the power of photosensitive response, which in turn depends on linear effect (polarizability,  $\alpha$ ) and nonlinear effect (hyperpolarizabilities,  $\beta$  and  $\gamma$ , etc.).

Therefore, unfolding of NLO response of (DPTM-1 to DPTM-12), the nonlinear and linear factors are estimated using (B3LYP) level with 6-31G (d, p) basis set. The  $\langle\alpha\rangle$  values in **Table 4** describe the effect of  $\pi$ -linkers on NLO and linear properties of

**TABLE 2** | Ionization potential (*IP*), electron affinity (*A*), electronegativity (*X*), global hardness (*η*), chemical potential (*μ*), global electrophilicity (*ω*), and global softness (*σ*) of entitled compounds (DPTM-1 to DPTM-12).

Dyes	<i>IP</i>	<i>A</i>	<i>X</i>	<i>η</i>	<i>μ</i>	<i>ω</i>	<i>σ</i>
DPTM-1	5.405	3.17	4.288	1.118	-4.288	8.22490	0.44743
DPTM-2	5.521	3.32	4.423	1.099	-4.423	8.90237	0.45517
DPTM-3	5.663	3.43	4.545	1.118	-4.545	9.23838	0.44723
DPTM-4	5.775	3.57	4.675	1.101	-4.675	9.92774	0.45434
DPTM-5	5.342	3.17	4.258	1.084	-4.258	8.36281	0.46126
DPTM-6	5.405	3.34	4.373	1.032	-4.373	9.26508	0.48449
DPTM-7	5.604	3.44	4.521	1.083	-4.521	9.43649	0.46168
DPTM-8	5.645	3.61	4.627	1.019	-4.627	10.5079	0.49092
DPTM-9	5.496	3.11	4.304	1.192	-4.304	7.77031	0.41946
DPTM-10	5.572	3.29	4.432	1.14	-4.432	8.61519	0.43859
DPTM-11	5.675	3.19	4.43	1.245	-4.43	7.88149	0.40161
DPTM-12	5.743	3.37	4.555	1.189	-4.555	8.72674	0.42069

**TABLE 3** | NBO charges for donor,  $\pi$ -linkers, and acceptor of the investigated compounds (DPTM-1 to DPTM-12).

Compounds	<b>D</b>	<b><math>\Pi</math></b>	<b>A</b>
DPTM-1	0.0886	0.1781	-0.2667
DPTM-2	0.1032	0.1277	-0.2309
DPTM-3	0.1567	0.0638	-0.2206
DPTM-4	0.1475	0.0150	-0.1893
DPTM-5	0.0579	0.2033	-0.2612
DPTM-6	0.0647	0.0029	-0.2252
DPTM-7	0.1336	0.0766	-0.2101
DPTM-8	0.0477	0.0379	-0.1780
DPTM-9	0.1823	0.1671	-0.2532
DPTM-10	0.0939	0.1236	-0.2175
DPTM-11	0.1455	0.0993	-0.2448
DPTM-12	0.1533	0.0558	-0.2191

entitled compounds. Polarizability is defined by a second rank tensor  $\langle\alpha\rangle$ . The  $\langle\alpha\rangle$  of the **R** observed is 645.71 *a.u.* (Khan et al., 2018a). Odd number of design compounds having 2,5-dimethylfuran as a second  $\pi$ -linker, the highest value of  $\langle\alpha\rangle$  is observed for **DPTM-5** (677.51 *a.u.*) with 5,5'-dimethyl-2,2'-bifuran as a conjugated first  $\pi$ -linker. This value lessens to 663.48 *a.u.* in **DPTM-1** containing 5-dimethylfuro[3,2-b]furan as a first  $\pi$ -linker; this value more decreases to 640.19 *a.u.* in **DPTM-3** having 2,5-dimethylloxazolo[5,4-d]oxazole as a first  $\pi$ -linker. In case of **DPTM-7**, **DPTM-9**, and **DPTM-11** the value of  $\langle\alpha\rangle$  further decreases to 625.88, 615.55, and 595.48 *a.u.* with 2,2'-dimethyl-5,5'-bioxazole, 2,5-dimethylbenzofuran, and 2,5-dimethylbenzo[d]oxazole first  $\pi$ -linker, respectively. In the same way, **DPTM-2**, **DPTM-4**, **DPTM-6**, **DPTM-8**, **DPTM-10**, and **DPTM-12** have 2,5-dimethylloxazole as a second  $\pi$ -linker. Among these compounds, **DPTM-6** comprises the highest value of  $\langle\alpha\rangle$  (668.19 *a.u.*) with 5,5'-dimethyl-2,2'-bifuran as a first  $\pi$ -linker. Moreover, this value decreases to 649.34, 629.01, 619.24, and 605.58 *a.u.* for **DPTM-2**, **DPTM-4**, **DPTM-8**, and **DPTM-10** comprising 2,5dimethylfuro[3,2-b]furan, 2,5-dimethylloxazolo [5,4-d]oxazole, 2,2'-dimethyl-5,5'-bioxazole, and **DPTM-2,5**-dimethylbenzofuran as first  $\pi$ -linker, respectively. The least

**TABLE 4** | Dipole polarizabilities and major contributing tensors (*a.u.*) of investigated compounds (DPTM-1 to DPTM-12).

Dyes	$\alpha_{xx}$	$\alpha_{yy}$	$\alpha_{zz}$	$\langle\alpha\rangle$
DPTM-1	1,323.91	410.25	256.28	663.48
DPTM-2	1,296.07	403.99	247.95	649.34
DPTM-3	1,277.01	399.33	244.23	640.19
DPTM-4	1,257.13	391.57	238.33	629.01
DPTM-5	1,318.15	443.99	270.4	677.51
DPTM-6	1,302.39	437.05	265.15	668.19
DPTM-7	1,188.82	429.51	259.3	625.88
DPTM-8	1,180.89	422.08	254.75	619.24
DPTM-9	1,056.67	524.27	265.72	615.55
DPTM-10	1,054.02	500.93	261.8	605.58
DPTM-11	1,025.84	497.34	263.25	595.48
DPTM-12	1,018.02	477.17	257.21	584.13

**TABLE 5** | The computed ( $\beta_{total}$ ) and major contributing tensor (*a.u.*) of the investigated compounds (DPTM-1 to DPTM-12).

Compounds	$\beta_{xxx}$	$\beta_{xyy}$	$\beta_{zzz}$	$\beta_{yzz}$	$\beta_{total}$
DPTM-1	88,934.67	2,873.69	-28.12	7.81	89,578.00
DPTM-2	-100109.29	2,981.49	31.01	11.49	99,533.83
DPTM-3	-94343.73	1879.08	38.68	4.49	93,827.84
DPTM-4	102,085.60	1743.79	83.78	11.84	101,482.89
DPTM-5	93,151.97	3,530.22	-25.63	-24.78	92,976.03
DPTM-6	110,721.70	4,090.21	-35.03	-14.06	110,509.23
DPTM-7	-83665.39	1725.26	65.38	-15.44	83,266.12
DPTM-8	100,162.89	2048.58	-75.11	-4.89	99,698.28
DPTM-9	-56590.14	3,357.43	10.1	23.65	59,359.72
DPTM-10	-68463.82	3,808.97	4.28	30.35	70,986.62
DPTM-11	-47174.53	1,662.33	-20.17	34.28	49,099.29
DPTM-12	-57330.71	1807.02	-9.32	31.52	58,930.08

value of  $\langle\alpha\rangle$  is observed in case of **DPTM-12** (584.13 *a.u.*) with 2,5-dimethylbenzo[d]oxazole as a first  $\pi$ -linker. **DPTM-5** showed an amplified value of  $\langle\alpha\rangle$  677.51 (*a.u.*), indicating a strong NLO effect, while **DPTM-12** molecule reveals retracted value of  $\langle\alpha\rangle$  584.13 *a.u.* The overall decreasing order of polarizability is **DPTM-5**>**DPTM-6**>**DPTM-1**>**DPTM-3**>**DPTM-4**>**DPTM-7**>**DPTM-8**>**DPTM-9**>**DPTM-10**>**DPTM-11**>**DPTM-12** (Table 4).

According to the literature, polarizability of a molecule is influenced by the energy bandgap between LUMO and HOMO. Small amounts of energy gap are required to demonstrate a high level of linear polarizability. Generally speaking, compounds with a small  $\Delta E$  and large  $\langle\alpha\rangle$  value suggest high  $\beta$  values (Qin and Clark, 2007). Electronic transitions along the *x* and *y* axes are commonly used to calculate polarizability. To illustrate dipole polarizability, Eq. 10 is utilized:

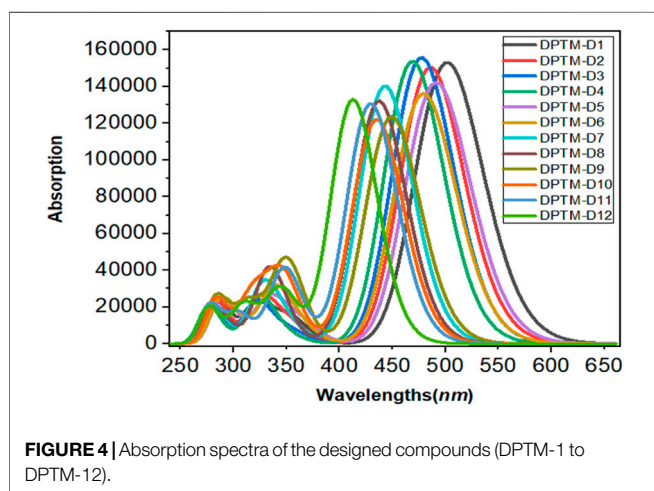
$$\alpha \propto \frac{(M_X^{gm})^2}{E_{gm}} \quad (10)$$

The transition moment is indicated as  $M_X^{gm}$  and transition energy between HOMO and LUMO is indicated as  $E_{gm}$ . This equation shows that  $\alpha$  is directly related to the square of transition moment

**TABLE 6** | Transition energy (eV), maximum absorption wavelengths ( $\lambda_{max}$ ), oscillator strengths ( $f_{os}$ ), light-harvesting efficiency (LHE), transition moment ( $M_X^{gm}$  a.u.), and major molecular orbital transitions of the designed compounds.

Compounds	$E$ (eV)	$\lambda_{max}(nm)$	$f_{os}$	LHE	$\mu_{gm}(a.u)$	Major MO transitions
DPTM-1	2.386	519.57	2.143	0.992	5.63	H-1L(20%), HL(71%)
DPTM-2	2.480	500.03	2.125	0.992	6.56	H-1L(30%), HL+1(46%)
DPTM-3	2.525	491.06	2.197	0.993	5.95	H-1L(26%), HL(63%)
DPTM-4	2.580	480.50	2.186	0.993	6.79	H-1L(24%), HL(61%)
DPTM-5	2.449	506.34	1.984	0.989	5.96	H-1L(28%), HL(60%)
DPTM-6	2.524	491.26	1.921	0.988	7.05	H-1L(27%), HL(55%)
DPTM-7	2.737	452.99	1.966	0.989	6.09	H-1L(43%), HL(40%)
DPTM-8	2.785	445.12	1.880	0.986	6.89	H-1L(35%), HL(43%)
DPTM-9	2.690	460.92	1.743	0.981	4.96	H-1L(35%), HL(54%)
DPTM-10	2.795	443.62	1.747	0.982	6.65	H-1L(29%), HL(53%)
DPTM-11	2.814	440.55	1.822	0.984	4.03	H-1L(48%), HL(42%)
DPTM-12	2.950	420.34	1.888	0.987	5.56	H-1L(42%), HL(41%)

H = HOMO, L = LUMO, H-1 = HOMO-1, etc.

**FIGURE 4** | Absorption spectra of the designed compounds (DPTM-1 to DPTM-12).

and has an inverse relation with  $E_{gm}$ . It is intimated that a molecule with a higher  $M_X^{gm}$  and lower  $E_{gm}$  value possesses the maximum value of  $\alpha$ , so it contains amplified hyperpolarizability value. Thus, in order to estimate desirable NLO properties of moieties, dipole polarizabilities are contemplated as computable measurements. NLO response of dyes with regard to the first-order hyperpolarizability is described in **Table 5**. The remaining first-order hyperpolarizability tensors are exhibited in the supplementary information (**Supplementary Table 26**).

A third rank tensor represents the first hyperpolarizability. The  $\beta_{total}$  of the **R** observed is 66,275.95 a.u. (Khan et al., 2018a). Among all the compounds having 2,5-dimethylfuran as a second  $\pi$ -linker **DPTM-3** has the highest value of  $\beta_{total}$  (93,827.84 a.u.) with 2,5-dimethyloxazolo[5,4-d]oxazole as first  $\pi$ -linker. This value then decreases to 92,976.03 a.u. in **DPTM-5** that further diminishes to 85,798 a.u. in **DPTM-1**. A decrease in the  $\beta_{total}$  occurs from **DPTM-7** to **DPTM-9** and **DPTM-11**, with 83,266.12, 59,359.72, and 49,099.29 a.u. Similarly in the compounds having 2,5-dimethyloxazole as a second  $\pi$ -linker, **DPTM-6** is observed with the highest value of  $\beta_{total}$  (110,509.23 a.u.) and the least value is observed in **DPTM-12** (58,930.08 a.u.). The overall increasing order for  $\beta_{total}$  of all

entitled dyes is **DPTM-11**<**DPTM-12**<**DPTM-9**<**R**<**DPTM-10**<**DPTM-7**<**DPTM-1**<**DPTM-5**<**DPTM-3**<**DPTM-2**<**DPTM-8**<**DPTM-4**<**DPTM-6** (**Table 5**).

## UV-VISIBLE SPECTRAL ANALYSIS

UV-Vis spectroscopy provides valuable information about electronic transitions, charge transfer, and contributing configurations of the molecule. TD-DFT computations were carried out in the gas phase to calculate the electronic excitation spectra of the investigated designed compounds DPTM-1 to DPTM-12 at CAM-B3LYP/6-311G+(d,p) level. The transition between HOMO and LUMO is the main focus of the UV spectra. Electronic transitions were pointed out through wavelength, frequency, and computed transition energy. During TD-DFT computations, the six lowest singlet transitions were studied (**Supplementary Tables 27–38**). The wavelength related to  $\lambda_{max}$  oscillator strength ( $f_{os}$ ), transition nature, transition moment ( $M_X^{gm}$  a.u.), light-harvesting efficiency (LHE), and computed transition energy (eV) values of DPTM-1 to DPTM-12 compounds are described in **Table 6** while the absorption band of entitled compounds is exhibited in **Figure 4**.

The maximum wavelength absorbed by all the studied compounds (DPTM-1 to DPTM-12) is in the visible region. The highest  $\lambda_{max}$  has been observed in **DPTM-1**, which is 519.57 nm. The highest  $\lambda_{max}$  value indicated that greater electronic transition occurred in **DPTM-1** dye from HOMO to LUMO orbital. All the investigated dyes have shown greater  $\lambda_{max}$  values from the **R** (430.50 nm) (Khan et al., 2018a) except the **DPTM-12**. From **Table 6**, it is apparent that the electron transitions of all dyes (except **DPTM-7**, **DPTM-11**, and **DPTM-12**) principally originate from TPA (H) to the DCV (L) along the  $x$  direction. In **DPTM-7**, **DPTM-11**, and **DPTM-12**, the charge transfer mainly occurs from H-1 to L. The decreasing order of  $\lambda_{max}$  is **DPTM-1**>**DPTM-5**>**DPTM-2**>**DPTM-6**>**DPTM-3**>**DPTM-4**>**DPTM-9**>**DPTM-7**>**DPTM-8**>**DPTM-10**> **DPTM-11**>**R**>**DPTM-12** (**Table 6**).

The optical efficiency is directly related to a factor named light-harvesting efficiency (LHE). A larger LHE value is linked to the higher photocurrent response of the compound and vice versa. **Eq. 11** used to represent LHE is (Nalwa, 2000)

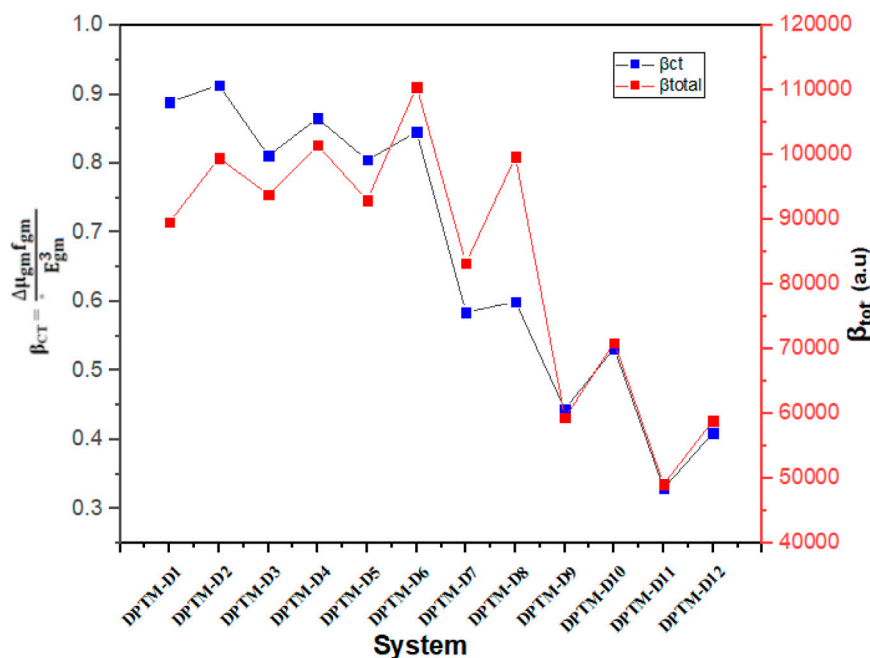


**FIGURE 5** | Relation between the  $\beta_{total}$  values and the consistent  $\beta_{CT}$  values of the investigated compounds (DPTM-1 to DPTM-12).

$$\text{LHE} = 1 - 10^{-f} \quad (11)$$

In Eq. 11,  $f$  stands for strength of oscillations. LHE of **DPTM-3** and **DPTM-4** is the highest among all the investigated compounds as given in **Table 6**. These calculations indicate a better connection between donor and acceptor units leading to a potential NLO response. Oudar and Chemla (Oudar and Chemla, 1977) presented the two-level models which explain the relationship between charge transfer transitions, and the first hyperpolarizability depends upon sum-over-states (SOS) relation showed in

$$\beta_{CT} = \frac{\Delta\mu_{gm} f_{gm}}{E_{gm}^3}. \quad (12)$$

In this expression,  $\beta_{CT}$  is the first hyperpolarizability,  $\Delta\mu_{gm}$  represents dipole moment difference,  $f_{gm}$  represents the strength of oscillation from the lower to higher state, and  $E_{gm}^3$  represents the cube of transition energy. The product of  $f$   $\Delta\mu_{gm}$  and  $f_{gm}$  is directly related to the first hyperpolarizability, while transition energy  $E_{gm}^3$  and first hyperpolarizability ( $\beta$ ) value have an inverse relation. So, NLO material with a higher  $\Delta\mu_{gm}$ ,  $f_{gm}$  value, and charge transfer of lower energy have an excellent NLO response with a large  $\beta$  value. The relation between the  $\beta_{total}$  and the constant  $\beta_{CT}$  of investigated compounds is manifested in **Figure 5**. It is evident from **Figure 5** that  $\beta_{tot}$  values are in good contract with the formula  $(\Delta\mu_{gm} f_{gm} / \Delta E_{gm}^3)$  values recommended by the two-level model. These conclusions indicate that using various  $\pi$ -bridges is an important methodology for designing new appealing D- $\pi$ -A structures with excellent NLO properties. This leads to NLO materials with an effective photoelectric and optical response.

## CONCLUSION

In summary, the objective of the present study was to investigate NLO properties of metal-free, theoretically designed organic dyes (DPTM-1 to DPTM-12) comprising of various  $\pi$ -linkers mixed with D and A. To elucidate the impact of various  $\pi$ -bridges on NLO properties, TD-DFT and DFT methods have been employed on designed dyes (DPTM-1 to DPTM-12). Electronic structures, absorption spectra, energy difference, and first hyperpolarizability values are explained by the quantum chemical methods. All dyes have shown maximum absorbance in the visible region, low transition energy, LHE, and oscillating strength values as compared to **R**. The highest red-shifted absorption spectra have been observed at 519.57 nm in **DPTM-1**. The NBO analysis explained the charge transfer mechanism from donor to acceptor part through the  $\pi$ -conjugated linkers. The highest NBO charge transfer was observed for **DPTM-1**. The FMO analysis illustrated electron density of all dyes, in HOMO electron density is primarily located on the DPA and first  $\pi$  linkers and in LUMO electron density is located at the DCV. Electron density transfer from the HOMO orbital to LUMO orbital plays an important role to enhance the NLO properties. The lowest HOMO to LUMO energy difference was observed for **DPTM-4**, **DPTM-6**, and **DPTM-8** with the lowest  $E_{gap}$  of 2.20, 2.06, and 2.04 eV, respectively. The greater amount of NLO properties was 101,482.89, 110,509.23, and 99,698.28 a.u. in **DPTM-4**, **DPTM-6**, and **DPTM-8**, respectively, with urea as a standard. The **DPTM-6**  $\beta_{tot}$  value is twenty-six hundred times greater than urea. Among all designed compounds these compounds exhibit lowest energy band gap and highest NLO response. This present work also depicted the importance of structural tailoring of  $\pi$ -linkers in D- $\pi$ -A dyes. It is a valuable theoretical approach for the researchers to design

new excellent NLO materials. This work also provided new ways to experimentally synthesize new appealing NLO materials for their use in optics and electronics devices.

## DATA AVAILABILITY STATEMENT

The original contributions presented in the study are included in the article/**Supplementary Material**; further inquiries can be directed to the corresponding authors.

## AUTHOR CONTRIBUTIONS

All authors listed have made a substantial, direct, and intellectual contribution to the work and approved it for publication.

## REFERENCES

- Afzal, Z., Hussain, R., Khan, M. U., Khalid, M., Iqbal, J., Alvi, M. U., et al. (2020). Designing Indenothiophene-Based Acceptor Materials with Efficient Photovoltaic Parameters for Fullerene-free Organic Solar Cells. *J. Mol. Model.* 26, 1–17. doi:10.1007/s00894-020-04386-5
- Amiri, S. S., Makarem, S., Ahmar, H., and Ashenagar, S. (2016). Theoretical Studies and Spectroscopic Characterization of Novel 4-Methyl-5-((5-Phenyl-1, 3, 4-Oxadiazol-2-Yl) Thio) Benzene-1, 2-diol. *J. Mol. Struct.* 1119, 18–24. doi:10.1016/j.molstruc.2016.04.053
- Anthony, J. K., Kim, H. C., Lee, H. W., Mahapatra, S. K., Lee, H. M., Kim, C. K., et al. (2008). Particle Size-dependent Giant Nonlinear Absorption in Nanostructured Ni-Ti Alloys. *Opt. Express* 16, 11193–11202. doi:10.1364/oe.16.011193
- Berkovic, G., Shen, Y. R., and Shadt, M. (1987). The Effect of Conjugation Length and Electron Donor Groups on the Second Order Nonlinear Polarizability of Cyano Substituted Aromatic Molecules. *Mol. Crystals Liquid Crystals Incorporating Nonlinear Opt.* 150, 607–616. doi:10.1080/00268948708074818
- Bilal Ahmed Siddique, M., Hussain, R., Ali Siddique, S., Yasir Mehboob, M., Irshad, Z., Iqbal, J., et al. (2020). Designing Triphenylamine-Configured Donor Materials with Promising Photovoltaic Properties for Highly Efficient Organic Solar Cells. *ChemistrySelect* 5, 7358–7369. doi:10.1002/slct.202001989
- Breitung, E. M., Shu, C.-F., and McMahon, R. J. (2000). Thiazole and Thiophene Analogues of Donor–Acceptor Stilbenes: Molecular Hyperpolarizabilities and Structure–Property Relationships. *J. Am. Chem. Soc.* 122, 1154–1160. doi:10.1021/ja9930364
- Chattaraj, P. K., Giri, S., and Duley, S. (2011). Update 2 of: Electrophilicity Index. *Chem. Rev.* 111, PR43–PR75. doi:10.1021/cr100149p
- Christodoulides, D. N., Khoo, I. C., Salamo, G. J., Stegeman, G. I., and Van Stryland, E. W. (2010). Nonlinear Refraction and Absorption: Mechanisms and Magnitudes. *Adv. Opt. Photon.* 2, 60–200. doi:10.1364/aop.2.000060
- Civalleri, B., Zicovich-Wilson, C. M., Valenzano, L., and Ugliengo, P. (2008). B3LYP Augmented with an Empirical Dispersion Term (B3LYP-D\*) as Applied to Molecular Crystals. *Cryst. Eng. Comm.* 10, 405–410. doi:10.1039/b715018k
- Dalton, L. (2002). “Nonlinear Optical Polymeric Materials: From Chromophore Design to Commercial Applications,” in *Polymers for Photonics Applications I* (Springer), 1–86. doi:10.1007/3-540-44608-7\_1
- Dalton, L. (2001). “The Role of Nonlinear Optical Devices in the Optical Communication Age,” in *Nonlinear Optics for the Information Society* (Springer), 1. doi:10.1007/978-94-015-1267-1\_1
- Datta, A., and Pal, S. (2005). Effects of Conjugation Length and Donor-Acceptor Functionalization on the Non-linear Optical Properties of Organic Push-Pull Molecules Using Density Functional Theory. *J. Mol. Struct. THEOCHEM* 715, 59–64. doi:10.1016/j.theochem.2004.10.054

## FUNDING

Funding in the Lu lab was provided by the Fundamental Research Funds for the Central Universities (2232021G-04) and Shanghai Science and Technology Committee (19ZR1471100). MI expresses his appreciation to the Deanship of Scientific Research at King Khalid University, Saudi Arabia, for funding through research groups program under grant number R.G.P. 1/318/42.

## SUPPLEMENTARY MATERIAL

The Supplementary Material for this article can be found online at: <https://www.frontiersin.org/articles/10.3389/fmats.2021.719971/full#supplementary-material>

- Dena, A. S. A., Muhammad, Z. A., and Hassan, W. M. J. C. P. (2019). Spectroscopic, DFT Studies and Electronic Properties of Novel Functionalized Bis-1, 3, 4-thiadiazoles. *Chem. Pap.* 73, 2803–2812. doi:10.1007/s11696-019-00833-7
- Drozd, M., and Marchewka, M. K. (2005). The Structure, Vibrational Spectra and Nonlinear Optical Properties of Neutral Melamine and Singly, Doubly and Triply Protonated Melaminium Cations-Theoretical Studies. *J. Mol. Struct. THEOCHEM* 716, 175–192. doi:10.1016/j.theochem.2004.11.020
- Dulic, A., Flytzanis, C., Tang, C. L., Pépin, D., Fétizon, M., and Hoppilliard, Y. (1981). Length Dependence of the Second-order Optical Nonlinearity in Conjugated Hydrocarbons. *J. Chem. Phys.* 74, 1559–1563. doi:10.1063/1.441296
- Eaton, D. F. (1991). *Nonlinear Optical Materials: The Great and Near Great*. Washington, DC: ACS Publications.
- Fukui, K. (1982). Role of Frontier Orbitals in Chemical Reactions. *science* 218, 747–754. doi:10.1126/science.218.4574.747
- Garza, A. J., Osman, O. I., Wazzan, N. A., Khan, S. B., Asiri, A. M., and Scuseria, G. E. (2014). A Computational Study of the Nonlinear Optical Properties of Carbazole Derivatives: Theory Refines experiment. *Theor. Chem. Acc.* 133, 1458. doi:10.1007/s00214-014-1458-9
- Gunasekaran, S., Balaji, R. A., Kumeresan, S., Anand, G., and Srinivasan, S. (2008). Experimental and Theoretical Investigations of Spectroscopic Properties of N-Acetyl-5-Methoxytryptamine. *Can. J. Anal. Sci. Spectrosc.* 53, 149–162.
- Haid, S., Marszalek, M., Mishra, A., Wielopolski, M., Teuscher, J., Moser, J.-E., et al. (2012). Significant Improvement of Dye-Sensitized Solar Cell Performance by Small Structural Modification in  $\pi$ -Conjugated Donor-Acceptor Dyes. *Adv. Funct. Mater.* 22, 1291–1302. doi:10.1002/adfm.201102519
- Hanwell, M. D., Curtis, D. E., Lonie, D. C., Vandermeersch, T., Zurek, E., and Hutchison, G. R. J. O. C. (2012). Avogadro: an Advanced Semantic Chemical Editor, Visualization, and Analysis Platform. *J. Cheminformatics* 4, 1–17. doi:10.1186/1758-2946-4-17
- Hochberg, M., Baehr-Jones, T., Wang, G., Shearn, M., Harvard, K., Luo, J., et al. (2006). Terahertz All-Optical Modulation in a Silicon-Polymer Hybrid System. *Nat. Mater.* 5, 703–709. doi:10.1038/nmat1719
- Hussain, R., Khan, M. U., Mehboob, M. Y., Khalid, M., Iqbal, J., Ayub, K., et al. (2020). Enhancement in Photovoltaic Properties of N, N -diethylaniline Based Donor Materials by Bridging Core Modifications for Efficient Solar Cells. *ChemistrySelect* 5, 5022–5034. doi:10.1002/slct.202000096
- Ivanov, I. P., Li, X., Dolan, P. R., and Gu, M. (2013). Nonlinear Absorption Properties of the Charge States of Nitrogen-Vacancy Centers in Nanodiamonds. *Opt. Lett.* 38, 1358–1360. doi:10.1364/ol.38.001358
- James, C., Raj, A. A., Reghunathan, R., Jayakumar, V. S., and Joe, I. H. (2006). Structural Conformation and Vibrational Spectroscopic Studies of 2,6-Bis(p-N,n-Dimethyl Benzylidene)cyclohexanone Using Density Functional Theory. *J. Raman Spectrosc.* 37, 1381–1392. doi:10.1002/jrs.1554
- Janjua, M. R. S. A. (2017). Nonlinear Optical Response of a Series of Small Molecules: Quantum Modification of  $\pi$ -spacer and Acceptor. *J. Iran Chem. Soc.* 14, 2041–2054. doi:10.1007/s13738-017-1141-x

- Karakas, A., Elmali, A., and Unver, H. (2007). Linear Optical Transmission Measurements and Computational Study of Linear Polarizabilities, First Hyperpolarizabilities of a Dinuclear Iron(III) Complex. *Spectrochimica Acta A: Mol. Biomol. Spectrosc.* 68, 567–572. doi:10.1016/j.saa.2006.12.029
- Khalid, M., Ali, A., Jawaria, R., Asghar, M. A., Asim, S., Khan, M. U., et al. (2020). First Principles Study of Electronic and Nonlinear Optical Properties of A-D- $\pi$ -A and D-A-D- $\pi$ -A Configured Compounds Containing Novel Quinoline-Carbazole Derivatives. *RSC Adv.* 10, 22273–22283. doi:10.1039/d0ra02857f
- Khalid, M., Ali, M., Aslam, M., Sumrra, S. H., Khan, M. U., Raza, N., et al. (2017). Frontier Molecular, Natural Bond Orbital, UV-Vis Spectral Study, Solvent Influence on Geometric Parameters, Vibrational Frequencies and Solvation Energies of 8-Hydroxyquinoline. *Int. J. Pharm. Sci. Res.* 8, 457. doi:10.13040/IJPSR.0975-8232.8(2).457-69
- Khan, M. U., Khalid, M., Ibrahim, M., Braga, A. A. C., Safdar, M., Al-Saadi, A. A., et al. (2018a). First Theoretical Framework of Triphenylamine-Dicyanovinylene-Based Nonlinear Optical Dyes: Structural Modification of  $\pi$ -Linkers. *J. Phys. Chem. C* 122, 4009–4018. doi:10.1021/acs.jpcc.7b12293
- Khan, M. U., Khalid, M., Ibrahim, M., Braga, A. A. C., Safdar, M., Al-Saadi, A. A., et al. (2018b). First Theoretical Framework of Triphenylamine-Dicyanovinylene-Based Nonlinear Optical Dyes: Structural Modification of  $\pi$ -Linkers. *J. Phys. Chem. C* 122, 4009–4018. doi:10.1021/acs.jpcc.7b12293
- Khoo, I. C. (2014). Nonlinear Optics, Active Plasmonics and Metamaterials with Liquid Crystals. *Prog. Quant. Elect.* 38, 77–117. doi:10.1016/j.pquantelec.2014.03.001
- Koopmans, T. (1934). Über die Zuordnung von Wellenfunktionen und Eigenwerten zu den Einzelnen Elektronen Eines Atoms. *physica* 1, 104–113. doi:10.1016/s0031-8914(34)90011-2
- Lesar, A., and Milošev, I. (2009). Density Functional Study of the Corrosion Inhibition Properties of 1,2,4-triazole and its Amino Derivatives. *Chem. Phys. Lett.* 483, 198–203. doi:10.1016/j.cplett.2009.10.082
- Mehboob, M. Y., Hussain, R., Khan, M. U., Adnan, M., Umar, A., Alvi, M. U., et al. (2020). Designing N-Phenylaniline-Triazole Configured Donor Materials with Promising Optoelectronic Properties for High-Efficiency Solar Cells. *Comput. Theor. Chem.* 1186, 112908. doi:10.1016/j.comptc.2020.112908
- Nalwa, H. S. (2000). *Handbook of Advanced Electronic and Photonic Materials and Devices, Ten-Volume Set*. Academic Press.
- Olson, J. K., and Boldyrev, A. I. (2012). Electronic Transmutation: Boron Acquiring an Extra Electron Becomes 'carbon'. *Chem. Phys. Lett.* 523, 83–86. doi:10.1016/j.cplett.2011.11.079
- Oudar, J. L., and Chemla, D. S. (1977). Hyperpolarizabilities of the Nitroanilines and Their Relations to the Excited State Dipole Moment. *J. Chem. Phys.* 66, 2664–2668. doi:10.1063/1.434213
- Parr, R. G., Donnelly, R. A., Levy, M., and Palke, W. E. (1978). Electronegativity: the Density Functional Viewpoint. *J. Chem. Phys.* 68, 3801–3807. doi:10.1063/1.436185
- Parr, R. G., Szentpály, L. v., and Liu, S. (1999). Electrophilicity index. *J. Am. Chem. Soc.* 121, 1922–1924. doi:10.1021/ja983494x
- Peng, Z., and Yu, L. (1994). Second-order Nonlinear Optical Polyimide with High-Temperature Stability. *Macromolecules* 27, 2638–2640. doi:10.1021/ma00087a039
- Prasad, P. N., and Williams, D. J. (1991). *Introduction to Nonlinear Optical Effects in Molecules and Polymers*. New York: Wiley.
- Qin, C., and Clark, A. E. (2007). DFT Characterization of the Optical and Redox Properties of Natural Pigments Relevant to Dye-Sensitized Solar Cells. *Chem. Phys. Lett.* 438, 26–30. doi:10.1016/j.cplett.2007.02.063
- Saeed, A., Muhammad, S., Rehman, S.-U., Bibi, S., Al-Sehemi, A. G., and Khalid, M. (2020). Exploring the Impact of central Core Modifications Among Several Push-Pull Configurations to Enhance Nonlinear Optical Response. *J. Mol. Graphics Model.* 100, 107665. doi:10.1016/j.jmngm.2020.107665
- Siddiqui, S. A., Rasheed, T., Faisal, M., Pandey, A. K., and Khan, S. B. (2012). Electronic Structure, Nonlinear Optical Properties, and Vibrational Analysis of Gemifloxacin by Density Functional Theory. *Spectrosc. Int. J.* 27. doi:10.1155/2012/614710
- Srinivasan, V., Panneerselvam, M., Pavithra, N., Anandan, S., Sundaravel, K., Jaccob, M., et al. (2017). A Combined Experimental and Computational Characterization of D- $\pi$ -A Dyes Containing Heterocyclic Electron Donors. *J. Photochem. Photobiol. A: Chem.* 332, 453–464. doi:10.1016/j.jphotochem.2016.09.026
- Sung, P.-H., and Hsu, T.-F. (1998). Thermal Stability of NLO Sol-Gel Networks with Reactive Chromophores. *Polymer* 39, 1453–1459. doi:10.1016/s0032-3861(97)85885-5
- Szafran, M., Komasa, A., and Bartoszak-Adamska, E. (2007). Crystal and Molecular Structure of 4-carboxypiperidinium Chloride (4-piperidinecarboxylic Acid Hydrochloride). *J. Mol. Struct.* 827, 101–107. doi:10.1016/j.molstruc.2006.05.012
- Tsutsumi, N., Morishima, M., and Sakai, W. (1998). Nonlinear Optical (NLO) Polymers. 3. NLO Polyimide with Dipole Moments Aligned Transverse to the Imide Linkage. *Macromolecules* 31, 7764–7769. doi:10.1021/ma9803436
- Vural, H., Orbay, M., and Ozdogan, T. J. B. Ö. K. (2017). A Combined Theoretical and Experimental Study of Cu (II) Complex with 2, 6-Pyridinedicarbonyl Dichloride, 132.
- Yamashita, S. (2011). A Tutorial on Nonlinear Photonic Applications of Carbon Nanotube and Graphene. *J. Lightwave Technol.* 30, 427–447. doi:10.1109/JLT.2011.2172574
- Yanai, T., Tew, D. P., and Handy, N. C. (2004). A New Hybrid Exchange-Correlation Functional Using the Coulomb-Attenuating Method (CAM-B3lyp). *Chem. Phys. Lett.* 393, 51–57. doi:10.1016/j.cplett.2004.06.011
- Zyss, J. (1987). "Quantum Electronics--Principles and Applications," in *Nonlinear Optical Properties of Organic Molecules and Crystals, Chapter II-1*. Editor D.S. Chemla (New York: Academic Press), 222–223.

**Conflict of Interest:** The authors declare that the research was conducted in the absence of any commercial or financial relationships that could be construed as a potential conflict of interest.

**Publisher's Note:** All claims expressed in this article are solely those of the authors and do not necessarily represent those of their affiliated organizations, or those of the publisher, the editors and the reviewers. Any product that may be evaluated in this article, or claim that may be made by its manufacturer, is not guaranteed or endorsed by the publisher.

Copyright © 2021 Khan, Khalid, Asim, Momina, Hussain, Mahmood, Iqbal, Akhtar, Hussain, Imran, Irfan, Ali, Rehman, Jiang and Lu. This is an open-access article distributed under the terms of the Creative Commons Attribution License (CC BY). The use, distribution or reproduction in other forums is permitted, provided the original author(s) and the copyright owner(s) are credited and that the original publication in this journal is cited, in accordance with accepted academic practice. No use, distribution or reproduction is permitted which does not comply with these terms.